Analytical Design Model for Reinforced Concrete Beams Strengthened in Shear Using L-Shaped CFRP Plates

Amir Mofidi[1], Omar Chaallal[2], and Yixin Shao[3]

Abstract

This paper presents the results of an analytical study on reinforced concrete (RC) T-beams strengthened in shear with L-shaped fiber-reinforced polymer (FRP) plates. The main objective of this study is to develop design equations for RC beams retrofitted in shear using L-shaped FRP plates, considering all possible modes of failure in ultimate limit states. Unlike RC beams strengthened with EB FRP plates and fabrics, prefabricated L-shaped plates feature unconventional failure modes due to their special shape and anchorage. The possible failure modes for RC beams strengthened with L-shaped FRP plates are: 1) Concrete breakout at the embedded part of the FRP plate in the flange; 2) FRP pull-off at the epoxy/FRP interface; 3) FRP pull-off at the concrete/epoxy interface; and 4) FRP overlap failure at the beam soffit. These failure modes do not occur in RC beams shear-strengthened with EB FRP fabrics and plates. Therefore, the existing design models for EB FRP fabrics and plates cannot predict with

[1] Postdoctoral Fellow, Department of Civil Engineering and Applied Mechanics, McGill University, 817 Sherbrooke West, Montreal QC Canada H3A 0C3. E-mail: amir.mofidi@mail.mcgill.ca

[2] Professor of Construction Engineering, University of Quebec, École de Technologie Supérieure, 1100 Notre-Dame West, Montreal QC Canada H3C 1K3 (corresponding author). E-mail: omar.chaallal@etsmtl.ca

[3] Associate Professor, Department of Civil Engineering and Applied Science, McGill University, Sherbrooke West, Quebec, Canada H3A 0C3. E-mail: yixin.shao@mcgill.ca

sufficient accuracy the contribution of FRP to the shear resistance of RC beams shear-strengthened with L-shaped plates. In this article, new design equations are proposed in light of recent developments and data. These equations distinguish the failure mode and calculate the FRP contribution to the shear resistance of RC beams strengthened with L-shaped FRP plates. In some cases, full embedment of the L-shaped CFRP plates in the RC beam flange is not feasible due to the presence of an obstacle (e.g., longitudinal reinforcing steel bars in the flange). The new design equations are applicable to RC beams strengthened with L-shaped FRP plates with different embedment lengths (including no embedment) of the CFRP plates in the RC beam flange. The proposed design equations are validated against experimental data collected from the literature.

CE Database subject headings: Concrete beam; Fiber-reinforced polymer; Strengthening; Shear; Epoxy bonding; Debonding; Embedment; L-shaped plates; Design equations.

INTRODUCTION

Recently, significant interest has been shown in the application of fiber-reinforced polymer (FRP) composites for strengthening and repair of existing reinforced concrete (RC) beams. During the past two decades, several valuable research studies have been completed on the shear-strengthening of RC beams with FRP composites using different methods. These methods include externally bonded (EB) FRP sheets, near-surface mounted (NSM) FRP rods, and embedded-through section (ETS) FRP rods (e.g., Uji 1992; Chaallal *et al.* 1998; Khalifa *et al.* 1998; Triantafillou 1998; De Lorenzis and Nanni 2001; Galal and Mofidi 2010; Chaallal *et al.* 2011). Meanwhile, to obtain a better insight into the behavior of FRP sheets and rods bonded to

concrete members, a large number of pull-off tests have been conducted worldwide (e.g., Maeda *et al.* 1997; Brosens and van Gemert 1999; Blaschko 2003; Seracino *et al.* 2007a). This undertaking has been particularly valuable for shear-strengthening, where bonding is critical. Based on experimental results, several bond models have been proposed to predict the bond behavior of FRP/concrete joints for EB FRP sheets, NSM FRP rods, and ETS FRP rods (e.g., Neubauer and Rostásy 1997; Maeda *et al.* 1997; Chen and Teng 2001; Blaschko 2003; De Lorenzis 2004; Yao *et al.* 2005; Seracino *et al.* 2007b; De Lorenzis and Teng 2007; Mofidi *et al.* 2012a). The FRP/concrete bond models have helped researchers to propose design equations for RC beams strengthened in shear with FRP composites by means of EB FRP sheets, NSM FRP rods, and ETS FRP rods (e.g., Khalifa *et al.* 1998; Chen and Teng 2003; Monti and Liotta 2006; Rizzo and De Lorenzis 2009; Mofidi and Chaallal 2011a; Mofidi *et al.* 2012a). However, there are very few research studies on the behavior of Adhesively Post-installed Embedded (APE) FRP plates bonded to concrete members. In particular, to the authors' knowledge, no studies on the bond strength of L-shaped FRP plate/concrete joints are available, and few investigations have been carried out on the retrofit of RC beams in shear with L-shaped FRP plates.

Meier (1998) experimentally investigated the strength of L-shaped FRP/concrete joints. Experimental tests on RC beams strengthened with L-shaped plates under static and cyclic loadings have been reported in Czaderski (1998), EMPA report No. 116/7 (2002), Czaderski and Motavalli (2004), Robertson (2004), and Chen and Robertson (2004). Mofidi *et al.* (2013) reported the experimental results of shear-strengthened RC beams using FRP L-shaped plates with different embedment lengths of the L-shaped plates in the RC beams' flange.

EMPA Report No. 116/7 (2002) proposed a design equation to calculate the contribution of CFRP L-shaped plates to shear resistance. Based on the truss model, this report recommended

66 that the maximum tensile force in one CFRP L-shaped plate should be limited to 45 kN for the
67 specific type of plate used in their study. Existing design models for RC beams shear-
68 strengthened with externally bonded (EB) FRP flat plates, laminates or sheets are not applicable
69 to beams strengthened with L-shaped FRP plates. Indeed, unlike RC beams strengthened with
70 EB FRP plates and fabrics, prefabricated L-shaped plates feature unconventional failure modes
71 due to their special shape and anchorage. The possible failure modes for RC beams strengthened
72 with L-shaped FRP plates are: flange anchorage failure modes (i.e. failure due to concrete
73 breakout at the flange, CFRP plate pull-off from the flange at the concrete/epoxy interface or
74 epoxy/FRP interface) and FRP overlap debonding failure mode. These failure modes do not
75 occur in RC beams shear-strengthened with FRP fabrics and plates. The main objective of this
76 study is to propose rational and accurate design equations to calculate the contribution of FRP to
77 shear resistance for different embedment lengths of L-shaped FRP plates and for all possible
78 failure modes of the strengthened RC beams.
79 In the current research study, a comprehensive, transparent, and rational design model has been
80 developed that incorporates different failure modes. These failure modes include: (1) concrete
81 breakout of the CFRP plate at the flange; (2) CFRP plate pull-off from the flange at the
82 epoxy/FRP interface; (3) CFRP plate pull-off from the flange at the concrete/epoxy interface; (4)
83 FRP plate debonding from the RC beam web and (5) debonding of the CFRP plate overlap at the
84 beam soffit. The results predicted using the proposed design equations are verified against the
85 experimental results presented by Mofidi *et al.* (2013) as well as those provided in EMPA Report
86 No. 116/7 (2002).
87
88 **Current Design Equations**

89 Czaderski and Motavalli (2004) used their own model proposed in EMPA Report No. 116/7
90 (2002) to predict the contribution of FRP to shear resistance for RC beams strengthened in shear
91 with L-shaped plates. According to their model, the nominal shear resistance at the ultimate limit
92 state, V_R, of RC beams retrofitted in shear with FRP L-shaped plates can be calculated simply by
93 adding the contribution of FRP, $V_{R,f}$, to that of concrete, $V_{R,c}$, and of steel, $V_{R,s}$, as follows:

94 $$V_R = V_{R,c} + V_{R,s} + V_{R,f} \ . \quad (1)$$

95 They recommended that, when calculating the state shear resistance at the ultimate limit, the
96 contribution of concrete to shear can be neglected. They also suggested that the maximum tensile
97 force in one CFRP L-shaped plate should be limited to 45 kN for the L-shaped plate that was
98 used in their study. Therefore, the ultimate limit-state shear resistance of RC beams strengthened
99 with L-shaped plates was expressed as follows (Czaderski and Motavalli 2004):

100 $$V_R = A_s . f_y . \frac{z_s}{s_s} . \cot\alpha + F_f \frac{z_f}{s_f} . \cot\alpha \quad \text{with: } F_f = 45 \text{ kN and } \alpha \geq 45° \ , \quad (2)$$

101 where A_s, f_y, z_s, s_s, α, F_f, z_f, and s_f are respectively the cross-sectional area, yield strength, and
102 internal lever arm strength of the transverse-steel reinforcement; the transverse-steel spacing; the
103 shear crack inclination; the tensile force in the FRP L-shaped plates; the internal lever arm
104 strength of the L-shaped FRP plates; and the spacing of the L-shaped plates. In their model, it
105 was assumed that the lever arm strengths for steel and for FRP transverse reinforcement were
106 equal.
107 Basically, the model used the strut-and-tie model for transverse FRP reinforcement, limiting the
108 strain in the FRP to 0.0067. The FRP strain limit calculations were performed based on the
109 characteristics of the L-shaped CFRP plate used, i.e., plate thickness t_f = 1.4 mm, plate width w_f
110 = 40 mm, and plate modulus of elasticity E_f = 120 GPa.

111 It has been established in recent years that many parameters affect the maximum tensile force
112 and the effective strain in externally bonded FRP plates (Triantafillou 1998; Chen and Teng
113 2001; Mofidi and Chaallal 2011a). By holding the maximum tensile force in the L-shaped FRP
114 plates constant, the effect of these influential parameters is thereby excluded (e.g., the concrete
115 compressive strength, the L-shaped plate dimensions and tensile characteristics, the bond
116 characteristics of the epoxy, and the groove dimensions in the flange). In addition, the equations
117 proposed in EMPA Report No. 116/7 (2002) are not applicable to beams strengthened using L-
118 shaped FRP plates with no or partial embedment of the CFRP plates in the beam flange.
119
120 **Proposed shear design equations**
121 In this section, new design equations are proposed for RC beams strengthened in shear using L-
122 shaped CFRP plates. The design model is capable of predicting the shear contribution of FRP for
123 specimens strengthened with different embedment lengths of CFRP L-shaped plates. Moreover,
124 it can predict the possible failure modes of the strengthened RC beams using L-shaped CFRP
125 plates.
126 For RC beams retrofitted with L-shaped CFRP plates, the FRP contribution to shear resistance
127 can be written in the following form:
128
$$V_f = \frac{2t_f \cdot w_f \cdot E_f \cdot \varepsilon_{fe} \cdot d_{fv}}{s_f} \quad (3)$$

129 where t_f, w_f, E_f, d_{fv}, ε_{ef}, and s_f are respectively the FRP plate thickness, FRP plate width, FRP
130 plate modulus of elasticity, effective shear depth of the cross section, effective strain in the FRP
131 plate, and spacing between the L-shaped CFRP plates. The effective shear depth can be taken as
132 the greater of 0.72h and 0.9d as per CSA/S806 (2012), where h and d are respectively the cross-

sectional height and effective depth of the RC beams. The FRP effective strain is the maximum strain experienced by the FRP at the ultimate point. Reliable predictions of the effective strains for all potential failure modes of the specimen constitute an important step towards achieving accuracy in calculating the FRP shear contribution at the ultimate loading stage. The maximum strain in the FRP plate on each side of a shear crack occurs at the location where the FRP has the greatest bond resistance. The corresponding effective strain in the FRP at the ultimate point due to the applicable failure modes should be evaluated on each side of the major shear crack. The failure occurs on the side with the lesser effective strain corresponding to an applicable failure mode. Therefore, the value of the lesser effective strain should be used in Eq. 3 to calculate the contribution of FRP to shear resistance.

Debonding of FRP sheets and plates is a common failure mode for RC beams strengthened using FRP sheets without end-anchorage or FRP plates without embedment of the FRP plate in the beam flange (Mofidi and Chaallal 2011b; Mofidi *et al.* 2012b). For retrofitted RC beams with partially or fully embedded L-shaped FRP plates, embedment failure of the FRP plates should be considered as a probable failure mode. The embedment failure of the CFRP plate in the RC beam flange can be due to: (i) concrete breakout failure, (ii) CFRP plate pull-off at the epoxy/FRP interface, or (iii) CFRP plate pull-off at the concrete/epoxy interface. Bond failure in the overlapping legs of the CFRP plates at the beam soffit can be another possible failure mode.

Failure due to debonding of CFRP plates from the web

For RC beams strengthened using L-shaped FRP plates with no embedment (similar to EB FRP U-jackets with no end anchorage), the bonding force developed in the FRP due to epoxy bonding

of the FRP plate or sheet to the web can be calculated using a model proposed by Mofidi and Chaallal (2011a) as follows:

$$P_{bond} = P_{max} \tag{4}$$

$$k_c\, k_L\, k_w\, L_e\, w_f\, \tau_{ef} = t_f\, w_f\, E_f\, \varepsilon_{fe} \ , \tag{5}$$

and hence:

$$\varepsilon_{fe-w} = \frac{k_c \cdot k_L \cdot k_w \cdot \tau_{ef} \cdot L_e}{t_f \cdot E_f} = 0.31 k_c . k_L . k_w \sqrt{\frac{\sqrt{f_c'}}{t_f E_f}} \le \varepsilon_{uf} \ , \tag{6}$$

where $\varepsilon_{fe\text{-}w}$, k_c, k_L, k_w, τ_{ef}, and L_e are respectively the effective strain in the FRP plate corresponding to the bond between the FRP plate or sheet to the RC beam web, the concrete-cracking coefficient based on transverse-steel and FRP rigidity values, a coefficient to compensate for insufficient FRP anchorage length, the FRP width-to-spacing ratio coefficient, the bond shear stress at failure, and the effective bond length. For details on calculations of k_c, k_L, and k_w, see Mofidi and Chaallal (2011a,b). The effect of transverse steel on the FRP contribution to shear resistance for RC beams shear-strengthened with L-shaped FRP plates was not investigated. Therefore, k_c is set to 1 in Eq. 6 in this article. Note that in any case, the effective strain in the FRP should not exceed the threshold of 0.006 to secure concrete integrity through aggregate interlocking mechanisms (*fib* 2001).

Failure due to concrete breakout at the flange:

Figure 1 presents possible embedment failure modes for CFRP plates bonded to the grooves in the concrete flange. Concrete breakout at the RC beam flange (Fig. 1-a) takes place when the CFRP plate develops a concrete failure cone. The failure occurs entirely in the concrete when the

stresses in the failure zone reach the concrete tensile strength. This failure mode can be more often expected in partially than in fully embedded CFRP plates.

Fuchs *et al.* (1995) proposed the concrete capacity design (CCD) approach for anchors in concrete, which included the behavioral model for concrete breakout failure. Considering the concrete-breakout failure mode, the model calculates the failure loads of cast-in-place or post-installed mechanical anchors in tension or in shear. The concrete-breakout model proposed by Fuchs *et al.* (1995) was later verified by Eligehausen *et al.* (2006) for anchors adhesively bonded to concrete. According to their model, the mean concrete breakout capacity for adhesively post-installed embedded anchors in an uncracked concrete (P_{fb}) can be calculated as follows:

$$P_{fb} = 14.7\sqrt{f_c'}(k_{el} \cdot L_{mb})^{1.5} \quad (7)$$

where f_c', k_{el}, L_{mb} are respectively the compressive strength of concrete in MPa, a coefficient to compensate for embedment lengths greater than the effective bond length of the plate, and the embedded length of the FRP plate in mm. Until further data on APE FRP plates bonded in concrete grooves are made available, Eq. 7 can be used to calculate the concrete breakout capacity of APE FRP plates. It is assumed that the bond stresses are uniformly distributed around the FRP-plate cross section. In Eq. 7, the embedded length of the FRP plates is limited to the effective bond length of the FRP plate. Since the concrete breakout failure mode takes place in concrete, this failure mode may seem not related the bond between the concrete and FRP. However, it should be noted that the tensile force applied to the FRP plate is transferred to concrete through the shear bond stresses along the APE FRP plate. This is when the concrete cone forms based on CCD model resulting thereby on a concrete breakout failure mode. According to the CCD model, there is a critical embedment depth, later termed the effective embedment depth, which plays an important role in forming the concrete cone (Fuchs et al. 1995). On the other hand, for APE FRP plates, the maximum length of the

197 embedded plate in the concrete that transfers the shear bond stresses is the effective bond length of
198 the FRP. Therefore, only the length of the APE FRP plate that is under bond stresses was used in the
199 CCD model. Obviously, the extra length of the APE FRP plate longer than the effective bond length
200 of FRP does not have a significant role in forming the concrete cone. It should be noted that similar
201 effective embedment lengths are considered in CCD model for other types of embedded anchors
202 and plates (see Fuchs. et al. 1995).

203 To this end, k_{el} is given by the following equations:

204
$$k_{el} = \begin{cases} 1 & \text{if } L_{mb} \le L_{ef} \\ L_{ef} \big/ L_{mb} & \text{if } L_{mb} > L_{ef} \end{cases}, \tag{8}$$

205 where L_{ef} is the effective bond length of the FRP plate. The effective bond length is the length
206 beyond which any increase in bond length does not translate into an increase in bond force. The
207 concept of effective bond length has been comprehensively discussed by many researchers for
208 externally-bonded FRP (EB FRP) plates and near-surface mounted (NSM) bars and plates (e.g.,
209 Neubauer and Rostásy 1997, Maeda *et al.* 1997, Chen and Teng 2001, De Lorenzis and Nanni 2001;
210 Mofidi and Chaallal 2011a). The equation to calculated the effective bond length for FRP plates
211 proposed by Neubauer and Rostásy (1997) shows good correlation with experimental results based
212 on direct pull-off tests of EB plates (Chen and Teng 2001). Neubauer and Rostásy (1997), and also
213 other researchers (e.g. Nakaba et al. 2001 and Ulaga et al. 2003), investigated experimentally the
214 bond behavior at the FRP/concrete interface FRP plates using double-lap tension tests. In these tests
215 the FRP plate is sandwiched/bonded between/to two concrete prisms. On the other hand, Meier
216 (1998) conducted pull-off test series on APE FRP epoxy bonded to concrete (Fig. 2). It can be seen
217 that APE FRP plated bonded to concrete grooves pullout test is very similar to double-lap tension

tests. Therefore, it was deemed reasonable to implement the equation proposed by Neubauer and Rostásy (1997) to calculate the effective length of APE FRP plates.

In addition, this article shows in the following sections that the equation proposed by Neubauer and Rostásy (1997) shows a reasonable correlation with experimental results based on direct pull-off tests of NSM plates. This indicates that the surrounding concrete does not influence the effective length of the FRP.

It should be mentioned that the effect of concrete confinement, although important for embedded FRP reinforcement (i.e. no epoxy bonding), may not have a significant effect on EB and APE FRP. Nevertheless, more experimental investigations are required to fully verify Eq. 9 for APE FRP plates bonded to concrete grooves.

Meanwhile and until further data is made available, Eq. 9 can be used to calculate L_{ef} for APE FRP plates in concrete:

$$L_{ef} = \sqrt{\frac{E_f \cdot t_f}{2\sqrt{f_{ct}}}} \ , \tag{9}$$

where f_{ct} is the concrete tensile strength, which can be calculated as a function of f_c' (Mirza *et al.* 1979) as follows:

$$f_{ct} = 0.53\sqrt{f_c'} \ . \tag{10}$$

Moreover, the FRP effective strain corresponding to the concrete breakout failure mode can be calculated using the equilibrium conditions in the FRP plate. Before concrete breakout, the force in the FRP plate is equal to the maximum tensile resistance in the concrete. In the case where failure is due to concrete breakout, the force developed in the FRP plate, P_{max}, can be calculated using Eq. 11:

$$P_{fb} = P_{max} = A_f \ . \ f_{ef} \ . \tag{11}$$

The effective FRP strain corresponding to the concrete breakout failure mode can be determined from the following equation:

$$\varepsilon_{ef-b} = \frac{14.7\sqrt{f_c'}(k_{el} \cdot L_{mb})^{1.5}}{t_f w_f E_f} \ . \quad (12)$$

Failure due to CFRP plate pull-off from the flange at the epoxy/FRP interface

Pull-off failure is a failure that occurs when the FRP plate or a part of the FRP plate slides out from the concrete (Fig. 1-b). In this mode, failure takes place mostly at the interface between the epoxy and the FRP plate. The maximum bond stress in this failure mode is basically a function of the shear strength of the epoxy and not of the concrete tensile strength.

Previous investigations have shown that the bond stress along embedded rods is nonlinearly distributed (e.g., De Lorenzis 2004; Eligehausen *et al.* 2004). However, it has been shown that the actual bond stress can be replaced by the maximum bond stress distributed along the effective bond length of the FRP rod or plate (McVay *et al.* 1996, Cook *et al.* 1998, Meszaros 1999; De Lorenzis and Teng 2007). In this failure mode, the maximum bond stress (τ_{max}) is associated with the mean bond strength of each epoxy product (τ_{af}). Therefore, the pull-off force of the CFRP plate from the flange at the epoxy/FRP interface (P_{fp}) can be calculated as follows:

$$P_{fp} = 2\tau_{\max}(t_f + w_f)k_{el}L_{mb} \ . \quad (13)$$

Blaschko (2003) proposed an equation to calculate the maximum bond stress of CFRP strips bonded into slits. The maximum bond stress for the embedded L-shaped CFRP plates failing due to pull-off at the epoxy/FRP interface is given by the following equations proposed by Blaschko (2003):

$$\tau_{\max} = 0.2\sqrt[4]{a_e'} \cdot \tau_{af} \le \frac{7.4\sqrt{f_c'}(k_{el} \cdot L_{mb})^{1.5}}{t_f + w_f} \ , \quad (14)$$

where a_e' is the lesser of the distances between the centerline of the groove to the edge of the concrete specimen or to the edge of the next groove, in millimeters, and τ_{af} is the shear strength of the epoxy in MPa. Note that the upper bound of the bond strength for the embedded CFRP plates is limited by the concrete pull-off strength.

Therefore, the effective FRP strain corresponding to CFRP plate pull-off at the epoxy/FRP interface can be calculated from the following equation:

$$\varepsilon_{ef-p} = \frac{0.4\sqrt[4]{a_e'} \cdot \tau_{af} \cdot k_{el} \cdot L_{mb}}{E_f}\left(\frac{1}{t_f} + \frac{1}{w_f}\right). \quad (15)$$

Failure due to CFRP plate pull-off from the flange at the concrete/epoxy interface:

According to previous experimental pull-off tests on EB and NSM FRP plates, rupture at the concrete/epoxy interface has been the major failure mode among all the failure modes considered (Chen and Teng 2001; Blaschko 2003; Yao *et al.* 2005; Seracino *et al.* 2007a). Failure at the concrete/epoxy interface is characterized by cracking in the concrete layer adjacent to the epoxy-bonded layer (Fig. 1-c). The FRP plate ultimately debonds from the concrete surface with a thin layer of the concrete (in some cases, only mortar with no aggregate attached to the FRP). Most experimental studies have been based on direct pull-off tests of EB FRP rods and plates or NSM FRP rods or strips. Several analytical and experimental bond models have been proposed for EB FRP rods and plates or NSM FRP rods or strips (e.g., Neubauer and Rostásy 1997; Maeda *et al.* 1997; Chen and Teng 2001; De Lorenzis 2004; De Lorenzis and Teng 2007). To the authors' knowledge, no bond models exist that are applicable to APE FRP plates in concrete grooves.

Among the bond models mentioned, that proposed by Seracino *et al.* (2007b) model is applicable to both EB and NSM FRP plates. According to Seracino *et al.* (2007b), their analytical model, which uses a linear softening bond-slip relationship, is applicable to any adhesively bonded plate and material. In this article, slight modifications were made to the Seracino *et al.* (2007b) model to make it completely applicable to APE FRP plates bonded to concrete. Therefore, the pull-off force of the CFRP plate from the flange at the concrete/epoxy interface (P_{fc}) can be calculated based on the Seracino *et al.* (2007b) model as follows:

$$P_{fc} = 0.85\varphi_f^{0.25} \cdot f_c'^{0.33}\sqrt{L_{per}E_f A_f} \quad , \tag{16}$$

where φ_f is the debonding-failure plane aspect ratio and is equal to d_f/b_f. In the calculation of φ_f, b_f is the length of the failure plane parallel to the concrete surface, which for NSM plates is taken to be the width of the groove + 2 mm. In addition, d_f is the length of the failure plane perpendicular to the concrete surface, which for NSM plates is taken to be the depth of the groove + 1 mm. This formula is modified for APE FRP plates to be the depth of the groove + 2 mm (Fig. 3).

Furthermore, L_{per} is the debonding failure plan in cross section, which is here taken to be $2(d_f + b_f)$ for APE plates. The proposed equation to calculate the pull-off force of the CFRP plate at the concrete/epoxy interface (Eq. 16) assumes that the effective length of the CFRP plate is fully available. The pull-off force of the CFRP plate at the concrete/epoxy interface is a linear function of the embedment length, where the effective length represents the upper bound of the FRP bond length (Oehlers and Seracino 2004; Seracino *et al.* 2007a). Therefore, the following modifications can be made to include the effect of effective bond length on the model:

$$P_{fc} = \frac{0.85k_{el} \cdot L_{mb} \cdot \varphi_f^{0.25} \cdot f_c'^{0.33}\sqrt{L_{per}E_f A_f}}{L_{ef}} . \tag{17}$$

304 It follows that the effective FRP strain corresponding to the CFRP plate pull-off at the
305 concrete/epoxy interface is:

306 $$\varepsilon_{ef-c} = \frac{0.85 k_{el} \cdot L_{mb} \cdot \varphi_f^{0.25} \cdot f_c'^{0.33} \sqrt{L_{per}}}{L_{ef} \sqrt{E_f A_f}}. \quad (18)$$

307 The effective length of the NSM FRP plates based on Seracino *et al.* (2007b) is given by the
308 following equations:

309 $$L_{ef} = \frac{\pi}{2\lambda} \; ; \qquad \lambda^2 = \frac{\tau_{\max} L_{per}}{\delta_{\max} E_f A_f} \quad (19)$$

310 $$\tau_{\max} = (0.802 + 0.078\varphi_f) f_c'^{0.6} \; ; \quad \delta_{\max} = \frac{0.976\varphi_f^{0.526}}{0.802 + 0.078\varphi_f} \; , \quad (20)$$

311 where λ is a constant, and τ_{max} and δ_{max} are respectively the maximum shear stress and the
312 maximum slip, assuming a bilinear bond-slip relationship at the concrete/epoxy interface. The
313 maximum shear stress and the maximum slip are calculated on the basis of an empirical equation
314 extracted from a statistical analysis.
315 The results of the equations proposed by Seracino *et al.* (2007b) to calculate the effective bond
316 length of NSM plates are compared with those from the equations proposed by Neubauer and
317 Rostásy (1997) to calculate the effective bond length of EB FRP plates (Eq. 9). The results of
318 experimental studies using push-pull tests on NSM FRP strip-to-concrete joints by Seracino *et al.*
319 (2007a) were compared with the calculated effective lengths for each specimen, using the
320 equations just mentioned. Figure 4 shows that the results calculated by the Seracino *et al.*
321 (2007b) and the Neubauer and Rostásy (1997) models are in good agreement with each other
322 (R^2=0.88). In this article, the equations by Neubauer and Rostásy (1997), which assume a
323 bilinear shear-slip model for FRP plates bonded to concrete (similarly to the assumption in

Seracino *et al.* 2007b), are used to determine the effective bond length. It is thought that the Neubauer and Rostásy (1997) model offers a more direct approach to the calculation of effective bond length than the Seracino *et al.* (2007b) model.

Failure due to debonding of overlapping CFRP plates from the soffit

Debonding of overlapping CFRP plates at the soffit of an RC beam shear-strengthened with L-shaped FRP plate is one possible failure mode. The development length of the L-shaped FRP plates bonded to the beam soffit (L_{dv}) should be determined so as to prevent debonding of the CFRP plate overlap.

Although the bond stress along the leg of the L-shaped plate bonded to the web is nonlinearly distributed, the actual bond stress can be replaced by the maximum bond stress distributed along the effective bond length of the FRP plate. In this way, the effect of the leg of the L-shaped plate bonded to the beam soffit can be considered to distribute the bond stresses linearly through the bond between the leg of the CFRP plate and the beam soffit. This translates into an increase in the effective bond area of the CFRP plate. Therefore, the bond strength can be calculated by introducing the effective bond area of the CFRP plate (Fig. 5), and the load required to debond the CFRP plate overlap from the beam soffit (P_{fo}) can be calculated as follows:

$$P_{fo} = [L_e \cdot \min(L_{dv}, L_e) - 0.5(L_e - w_f)(\min(L_{dv}, L_e) - w_f)] \cdot \tau_{ef}\,, \tag{21}$$

where τ_{ef} can be equated to the concrete tensile strength (f_{ct}). The effective FRP strain corresponding to overlap debonding of the CFRP L-shaped plate from the beam soffit can be calculated using the following equation:

$$\varepsilon_{fe-o} = \frac{[L_e \cdot \min(L_{dv}, L_e) - 0.5(L_e - w_f)(\min(L_{dv}, L_e) - w_f)] \cdot \tau_{ef}}{2 t_f E_f w_f}. \tag{22}$$

346 Note that the effective strain in the FRP plate at ultimate load can be calculated as:

347 $$\varepsilon_{fe-u} = \min(\varepsilon_{fe-w} + \min(\varepsilon_{fe-b}, \varepsilon_{fe-p}, \varepsilon_{fe-c}), \varepsilon_{fe-o}) . \quad (23)$$

348

349 **Verification of the proposed design proposals**

350 Currently, few pullout tests have been performed on APE FRP plates bonded to concrete grooves
351 or to shear-strengthened RC beams using L-shaped FRP plates. As previously mentioned, Meier
352 (1998) conducted a direct pullout test series on APE FRP plates bonded to concrete grooves (Fig.
353 2-a) and on L-shaped plates bonded to concrete block joints (Fig. 2-b). In this article, the
354 experimental results proposed by Meier (1998) are compared with the calculated results based on
355 the proposed equations (see Table 1). The calculated values of the pullout strength of FRP plates
356 corresponding to each failure mode are shown in Table 1. The failure mode of each specimen
357 was determined based on the corresponding calculated pullout force. Moreover, the results of the
358 pullout tests described by Meier (1998) on L-shaped CFRP plate joints bonded to concrete
359 blocks are compared with the results extracted from the proposed equations. Clearly, more
360 experimental data are needed to perform a full validation of the proposed equations.
361 Nevertheless, the predicted results for the pullout strength of APE FRP plates bonded to concrete
362 grooves and of L-shaped FRP plates bonded to concrete blocks show a good correlation with the
363 experimental results (R^2 = 0.98).
364 In another investigation, the experimental contributions of FRP to the shear resistance of the
365 retrofitted specimens in this study were compared with the shear resistance predicted by the
366 proposed equations (see Table 2). The calculated values of effective strain developed in the FRP
367 plates corresponding to each failure mode are shown in Table 2. The prevalent failure mode can
368 thus be identified. The FRP shear contribution was then calculated based on the critical effective

strain of the governing failure mode. Finally, the experimental results reported by Mofidi *et al.* (2013) and EMPA (2002) on RC beams shear-strengthened with L-shaped FRP plates are compared to the results calculated using the proposed equations (see Table 2). It should be noted that the shear resistance of the FRP corresponding to the calculated flexural failure load ($V_{f\text{-}flx}$) should be considered for the specimens that failed in flexure (S1-LS-FE and S4-EMPA). Overall, the calculated results show a reasonable correlation with the experimental results ($R^2 = 0.69$).

CONCLUSIONS

Based on the results of the current research study, the following major conclusions can be drawn:

- Comprehensive design equations for RC beams strengthened in shear with L-shaped FRP plates are proposed. These equations consider various potential failure modes, including: (1) concrete breakout at the flange, (2) CFRP plate pull-off from the flange at the epoxy/FRP interface, (3) CFRP plate pull-off from the flange at the concrete/epoxy interface, (4) debonding of FRP plate from the RC beam web, and (5) debonding of the CFRP plate overlap at the beam soffit.
- The proposed design equations are expected to be applicable to any embedment length of L-shaped FRP plates into the flange of RC beams. The effective application of partially embedded L-shaped CFRP plates to shear-strengthen RC beams was verified based on the analytical design model.
- The predicted results of the design equations were validated using few available experimental results in the literature.

ACKNOWLEDGMENTS

The authors wish to acknowledge the support provided by the Natural Sciences and Engineering Research Council of Canada through a postdoctoral fellowship to Dr. Amir Mofidi and to Prof. Chaallal through a Discovery grant.

REFERENCES

Blaschko, M. (2003). Bond behavior of CFRP strips glued into slits. *Proceedings, 6th International Symposium on Fiber-Reinforced Polymer Reinforcement for Concrete Structures*, K.H. Tan (ed.), Singapore, 205–214.

Brosens, K. and Van Gemert, D. (1999). Anchorage design for externally bonded carbon-fiber polymer laminates, *Proceedings, 4th International Symposium on Fiber-Reinforced Polymer Reinforcement for Concrete Structures*, Baltimore, United States, 635–645.

Chaallal, O., Mofidi, A., Benmokrane, B., and Neale, K. (2011). Embedded through-section FRP rod method for shear strengthening of RC beams: performance and comparison with existing techniques. *Journal of Composites for Construction* 15(3), 374–383.

Chaallal, O., Nollet, M.J., and Perraton, D. (1998). Strengthening of reinforced concrete beams with externally bonded fiber-reinforced plastic plates: design guidelines for shear and flexure. *Can. J. Civil Eng.* 25(4), 692–704.

Chen, J. and Robertson, I. (2004). Test of cracked pre-stressed concrete T-beam retrofitted for shear using CFRP L-shaped plates. *University of Hawaii Research Report, UHM/CEE/04-06.*

Chen, J.F. and Teng, J.G. (2001). Anchorage strength models for FRP and steel plates bonded to concrete. *J. Struct. Eng.* 127(7), 784–791.

Chen, J.F. and Teng, J.G. (2003). Shear capacity of FRP-strengthened RC beams: FRP debonding. *Construction and Building Materials* 17(1), 27–41.

Cook, R.A., Kunz, J., Fuchs, W., and Konz, R.C. (1998). Behavior and design of single adhesive anchors under tensile load in uncracked concrete. *ACI Structural Journal* 95(1), 9–26.

Czaderski, C. (1998). Nachträgliche Schubverstärkung mit CFK-Winkeln. *Schweizer Ingenieur und Architekt (SI + A)* 43(22), 822–826 (in German).

Czaderski, C. and Motavalli, M. (2004). Fatigue behavior of CFRP L-shaped plates for shear strengthening of RC T-beams. *Composites: Part B* 35, 279–290.

De Lorenzis, L. (2004). Anchorage length of near-surface mounted fiber-reinforced polymer rods for concrete strengthening—analytical modeling. *ACI Struct. J.* 101(3), 375–386.

De Lorenzis, L. and Nanni, A. (2001). Shear strengthening of reinforced concrete beams with NSM fiber-reinforced polymer rods. *ACI Struct. J*. 98(1), 60–68.

De Lorenzis, L. and Teng, J.G. (2007). Near-surface mounted FRP reinforcement: an emerging technique for structural strengthening. *Composites: Part B* 38, 119–143.

EMPA Test Report 116/7 (2002). Shear strengthening with prefabricated CFRP L-shaped plates: test beams S1 to S6. *Eidgenössische Materialprüfungs- und Forschungsanstalt*, 79 pages.

Eligehausen, R., Appl, J.J., Lehr, B., Meszaros, J., and Fuchs, W. (2004). Tragverhalten und Bemessung von Befestigungen mit Verbunddübeln unter Zugbeanspruchung, Part 1: Einzeldübel mit großem Achs- und Randabstand. *Beton und Stahlbetonbau* 99(7), 561–571 (in German).

Eligehausen, R., Cook, R.A., and Appl, J. (2006). Behavior and design of adhesive bonded anchors. *ACI Structural Journal* 103(6), 822–831.

fib-TG 9.3 (2001). *Externally Bonded FRP Reinforcement for RC Structures*. International Federation for Structural Concrete, Lausanne, Switzerland.

Fuchs, W., Eligehausen, R., and Breen, J.E. (1995). Concrete capacity design (CCD) approach for fastening to concrete. *ACI Structural Journal* 92(1), 73–94.

Galal, K. and Mofidi, A., (2010), Shear strengthening of RC T-beams using mechanically anchored unbonded dry carbon fibre sheets. *J. of Performance of Constructed Facilities* 24(1), 31–39.

Khalifa, A., Gold, W.J., Nanni, A., and Aziz, A. (1998). Contribution of externally bonded FRP to shear capacity of RC flexural members. *J. Compos. Constr*. 2(4), 195–203.

Maeda, T., Asano, Y., Sato, Y., Ueda, T., and Kakuta, Y. (1997). A study on bond mechanism of carbon fiber sheet. *Proceedings, 3rd International Symposium on Non-Metallic (FRP) Reinforcement for Concrete Structures*, Sapporo, Japan, 1, 279–286.

McVay, M., Cook, R.A., and Krishnamurthy, K. (1996). Pullout simulation of post-installed chemically bonded anchors. *ASCE Journal of Structural Engineering* 122(9), 1016–1024.

Meier, H., (1998). CFK-Schubverstärkungselemente. *Schweizer Ingenieur und Architekt (SI + A)* 43(22), 819–821 (in German).

Meszaros, J. (1999). *Tragverhalten von Verbunddübeln im ungerissenen und gerissenen Beton*. Doctoral thesis, University of Stuttgart, Stuttgart, Germany (in German).

Mirza, S., MacGregor, J., and Hatzinikolas, M. (1979). Statistical descriptions of strength of concrete. *J. Struct. Div*. 105(6), 1021–1037.

Mofidi, A. and Chaallal, O., (2011a), Renforcement à l'effort tranchant des poutres en béton armé à l'aide de matériaux composites collés en surface: Avancées et perspectives pour la norme CSA-S806. *Can. J. Civil Eng.* 38, 556–569.

Mofidi, A. and Chaallal, O. (2011b). Shear strengthening of RC beams with externally bonded FRP composites: effect of strip-width to strip-spacing ratio. *Journal of Composites for Construction* 15(5), 732–742.

Mofidi, A., Chaallal, O., Benmokrane, B., and Neale, K.W. (2012a). Performance of end-anchorage systems for RC beams strengthened in shear with epoxy-bonded FRP. *Journal of Composites for Construction* 16(3), 322–331.

Mofidi, A., Chaallal, O., Benmokrane, B., and Neale, K.W. (2012b). Experimental tests and design model for RC beams strengthened in shear using the embedded through-section FRP method. *Journal of Composites for Construction* 16(5), 540–550.

Mofidi, A., Thivierge, S., Chaallal, O., and Shao, Y. (2013). Performance of Reinforced Concrete Beams Strengthened in Shear Using L-Shaped CFRP Plates - An Experimental Investigation. *Journal of Composites for Construction*, doi:10.1061/(ASCE)CC.1943-5614.0000398.

Monti, G. and Liotta, M. (2006). Tests and design equations for FRP strengthening in shear. *Construction and Building Materials* 21, 799–809.

Nakaba, K., Kanakubo, T., Furuta, T. and Yoshizawa, H. (2001). Bond Behavior between Fiber-reinforced Polymer Laminates and Concrete, *ACI Structural Journal*, 98(3), 359–367.

Neubauer, U. and Rostásy, F.S. (1997). *Design Aspects of Concrete Structures Strengthened with Externally Bonded CFRP Plates.* ECS Publications, Edinburgh, 109–118.

Oehlers, D.J. and Seracino, R. (2004). *Design of FRP and Steel-Plated Structures*. Elsevier Science, Oxford, United Kingdom.

Rizzo, A. and De Lorenzis, L. (2009). Behavior and capacity of RC beams strengthened in shear with NSM FRP reinforcement. *Constr. and Building Materials* 23, 1555–1567.

Robertson, I., Johnson, G.P., and Sharma, B. (2007). Shear retrofit of concrete T-beams using CFRP. *Proceedings, 8rd International Symposium on Fiber-Reinforced Polymers in Reinforced Concrete Structures*, Patras, Greece.

Seracino, R., Jones, N.M., Ali, M.S.M., Page, M.W., and Oehlers, D.J. (2007a). Bond strength of near-surface mounted FRP strip-to-concrete joints. *Journal of Composites for Construction* 11(4), 401–409.

Seracino, R., Raizal Saifulnaz, M.R., and Oehlers, D.J. (2007b). Generic debonding resistance of EB and NSM plate-to-concrete joints. *Journal of Composites for Construction* 11(1), 62–70.

Triantafillou, T.C. (1998). Shear strengthening of reinforced concrete beams using epoxy-bonded FRP composites. *ACI Struct. J.* 95(2), 107–115.

Uji, K. (1992). Improving shear capacity of existing reinforced concrete members by applying carbon fiber sheets. *Trans. Jpn. Concr. Institute* 14, 253–266.

Ulaga, T., Vogel, T. and Meier, U. (2003). Bilinear Stress–Slip Bond Model: Theoretical Background and Significance, Proc. of the 6th *Int. Symp. on* on FRP Reinforcement for Concrete Structures (FRPRCS-6), Vol. 1, pp. 153–162.

Yao, J., Teng, J.G., and Chen, J.F. (2005). Experimental study on FRP-to-concrete bonded joints. *Composites, Part B: Engineering* 36(2), 99–113.

514

515

516 Table 1 – Predicted results from proposed design equations versus experimental
517 pullout results reported by Meier (1998).

Direct pullout test type	Bond length, mm^2	Experimental load at failure, kN	Predicted concrete breakout load, kN	Predicted pull-off load at epoxy/FRP interface, kN	Predicted pull-off load at concrete/epoxy interface, kN	Predicted overlap debonding load, kN
APE CFRP plate/concrete block joint	100	77.0	84.5	166.3	<u>70.3</u>	-
	150	100.0	126.2	249.7	<u>105.5</u>	-
	200	121.0	190.4	285.8	<u>121.0</u>	-
L-shaped CFRP plate/concrete block joint	150	67.0	-	-	-	<u>56.3</u>
	225	69.0	-	-	-	<u>63.5</u>
	300	74.0	-	-	-	<u>63.5</u>
						R^2=0.98

518 Note: The underlined failure load is the calculated governing failure load of
519 the FRP/concrete joint.

Table 2 – Summary of calculated results versus experimental results for shear-strengthened RC beams.

Specimen name/study	f_c', MPa	h, mm	h_f, mm	b_w, mm	d, mm	w_f, mm	t_f, mm	s_f, mm	E_f, GPa	ε_{fe-b}	ε_{fe-p}	ε_{fe-c}	ε_{fe-o}	ε_{fe-w}	ε_{fe-u}	V_{f-cal}, kN	V_{f-flx}, kN	V_{f-exp}, kN
S1-LS-NE Mofidi *et al.* 2013	33.7	406	102	152	350	40	2	187.5	90	0	0	0	0.058	0.018	0.018	<u>42.3</u>	12	59.2
S1-LS-PE Mofidi *et al.* 2013	33.7	406	102	152	350	40	2	187.5	90	0.015	0.054	0.024	0.058	0.018	0.033	<u>77.9</u>	12	84.1
S1-LS-FE Mofidi *et al.* 2013	33.7	406	102	152	350	40	2	187.5	90	0.119	0.216	0.096	0.058	0.018	0.058	138.9	<u>12</u>	119.5
S1-EB-NA Mofidi *et al.* 2013	33.7	406	102	152	350	n/a	0.107	n/a	231	0	0	0	0	0.048	0.048	<u>74.3</u>	12	77.8
S3 EMPA 2002	28.0	500	120	150	380	40	1.4	300.0	120	0.158	0.274	0.115	0.058	0.018	0.058	<u>89.1</u>	18	154.5
S4 EMPA 2002	30.8	500	120	150	380	40	1.4	300.0	120	0.158	0.274	0.115	0.058	0.018	0.058	89.1	<u>24.6</u>	17.0

Note: The underlined shear contribution of FRP is the V_f corresponding to the calculated governing failure mode of the beam.

ε_{fe-b}, ε_{fe-p}, ε_{fe-c}, ε_{fe-o}, ε_{fe-w}, and ε_{fe-u} are the effective FRP strains corresponding to concrete breakout, FRP pull-off at the epoxy/FRP interface, FRP pull-off at the concrete/epoxy interface, overlap debonding of the CFRP L-shaped plate, debonding of FRP from the web, and ultimate shear failure respectively. V_{f-cal}, V_{f-flx}, *and* V_{f-exp} are the FRP shear contributions corresponding to the calculated effective strain at ultimate load, the values at flexural failure of the beam, and experimental results respectively. The effective strain of the FRP at ultimate load is given by: $\varepsilon_{fe-u} = \min(\varepsilon_{fe-w} + \min(\varepsilon_{fe-b}, \varepsilon_{fe-p}, \varepsilon_{fe-c}), \varepsilon_{fe-o})$.

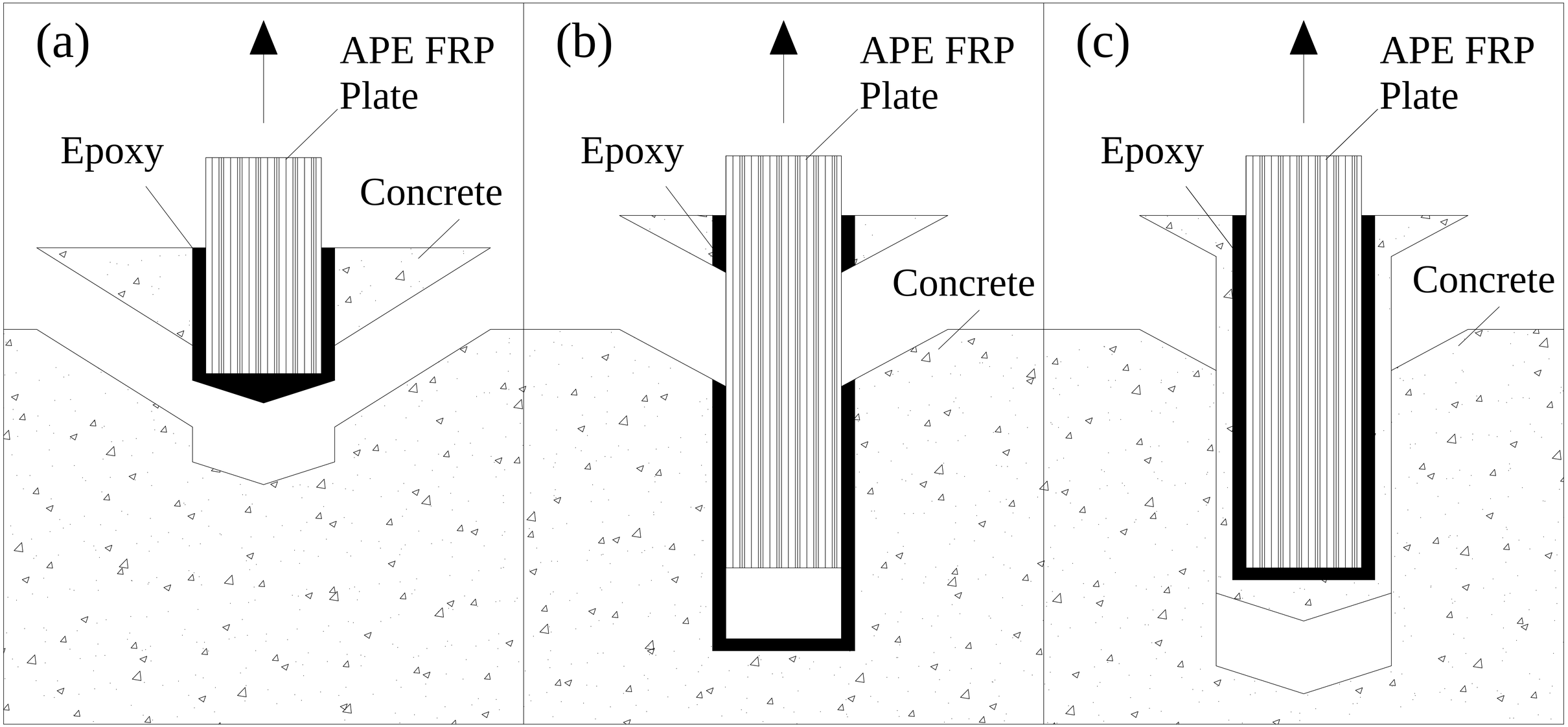
(a)
APE FRP
Plate
Epoxy
Concrete
(b)
APE FRP
Plate
Epoxy
Concrete
(c)
APE FRP
Plate
Epoxy
Concrete

(a)

APE FRP Plate

Epoxy

Concrete

L_{mb}

(b)

L-shaped FRP Plate

Epoxy

Concrete

L_{dv}

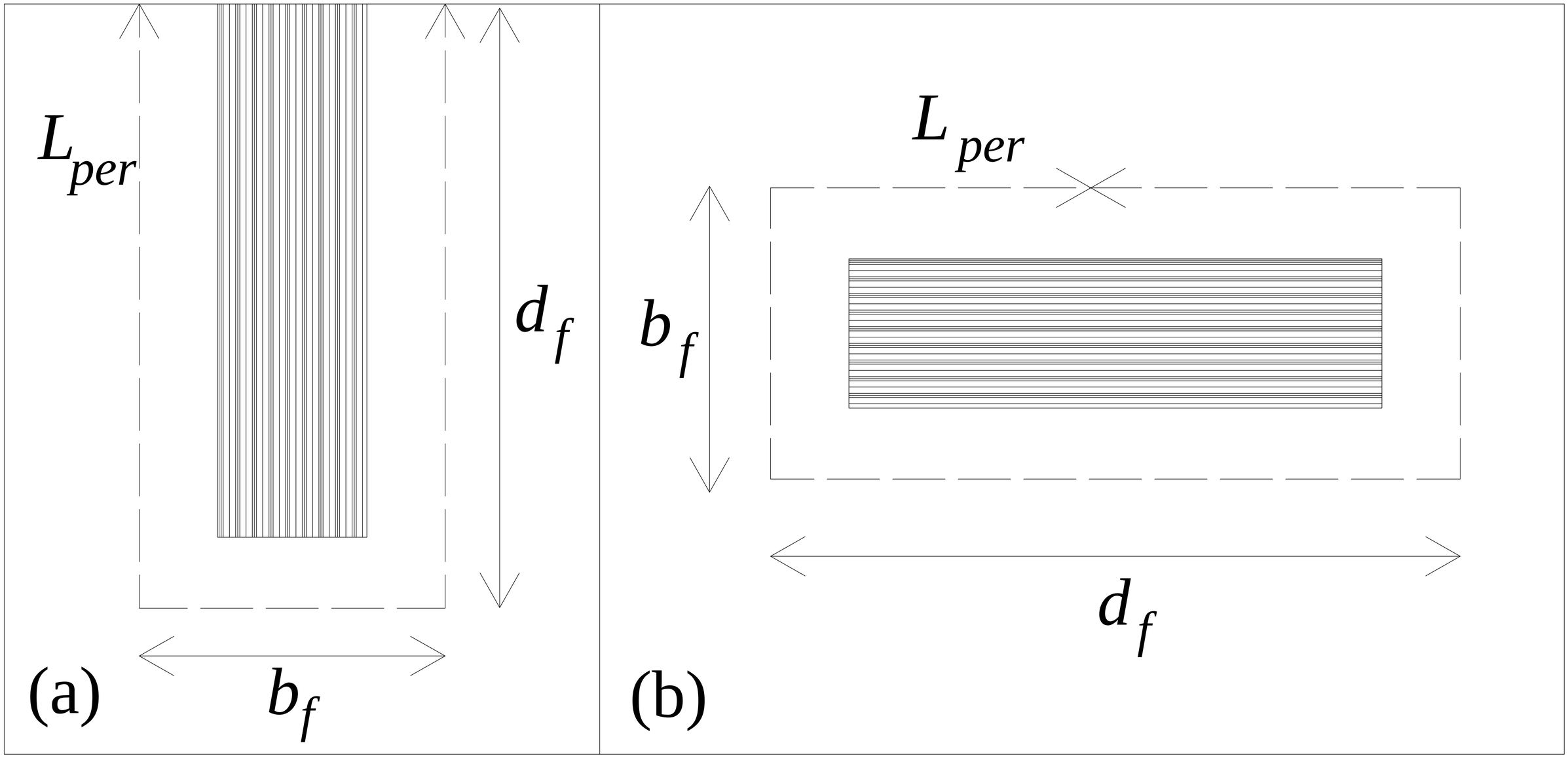
L_{per}
d_f
b_f
(a)
b_f
L_{per}
b_f
d_f
(b)

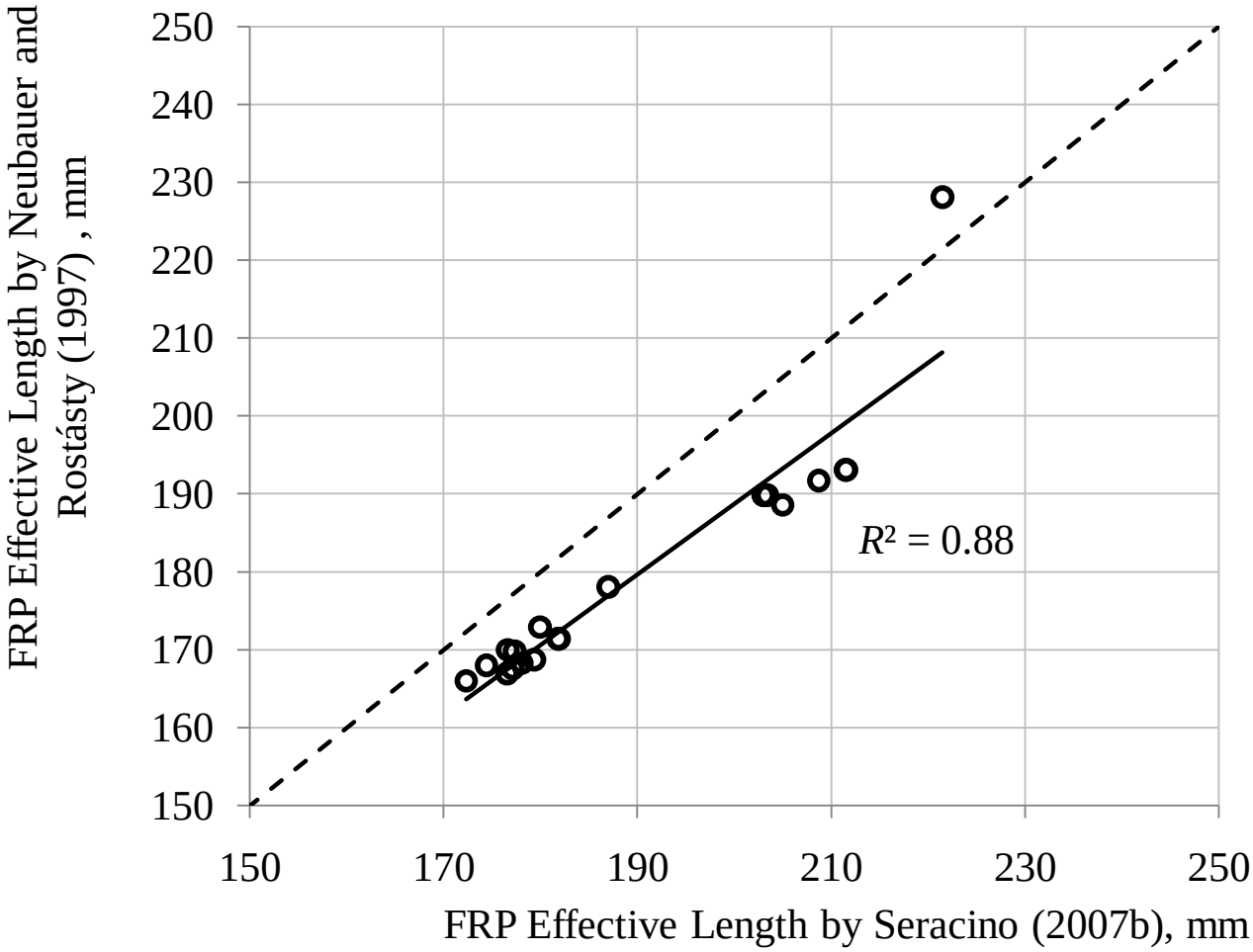
FRP Effective Length by Neubauer and Rostásty (1997) , mm
250
240
230
220
210
200
190
180
170
160
150
150
170
190
210
230
250
FRP Effective Length by Seracino (2007b), mm
R² = 0.88

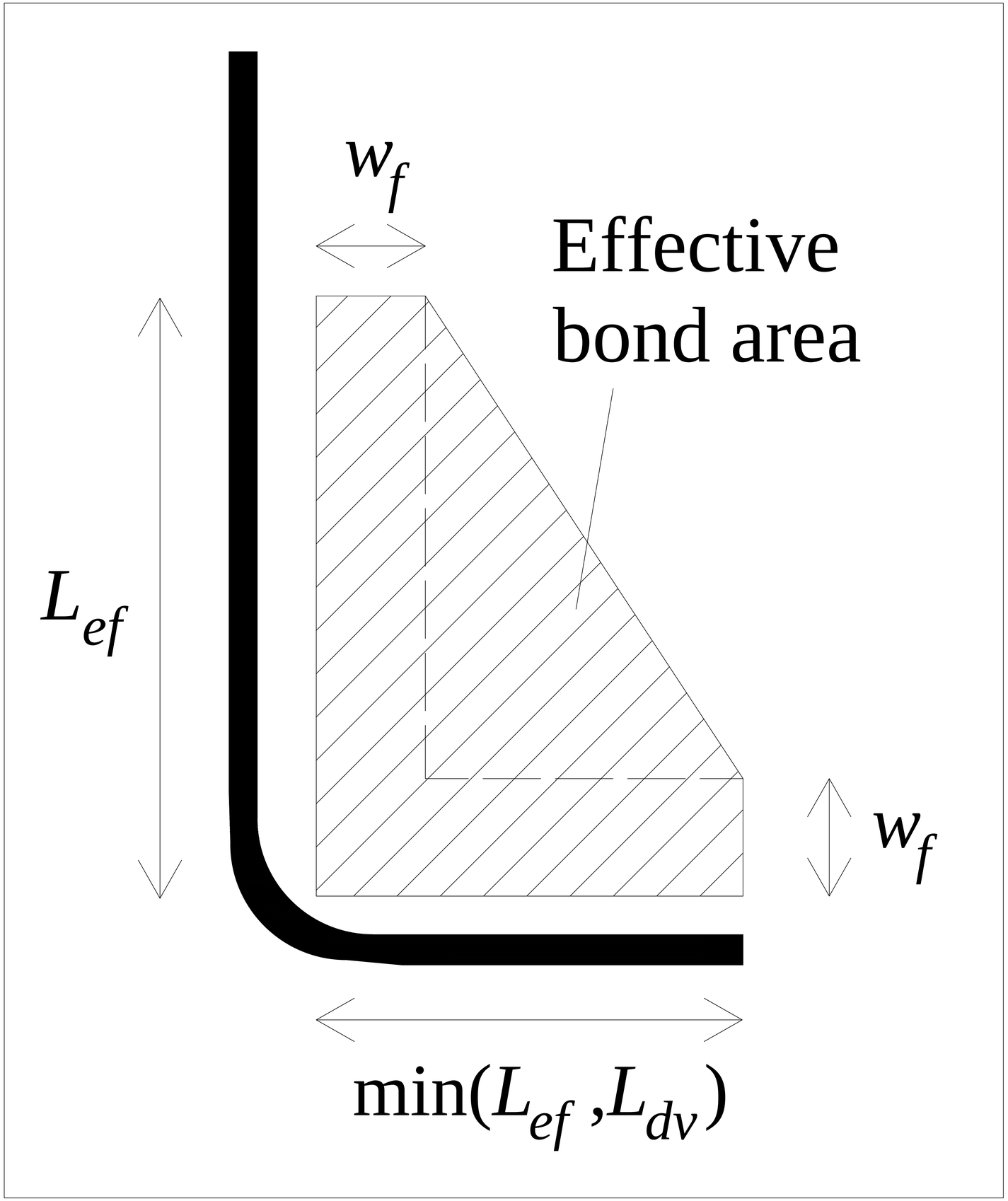
w_f
Effective
bond area
L_{ef}
w_f
$\min(L_{ef}, L_{dv})$